Analyticity, renormalization, and evolution of the soft-quark function

Xiang-Peng Wang

In collaboration with G. T. Bodwin, J. Ee and J. Lee: arXiv:2101.04872

Argonne National Laboratory

April 01, 2021

Outlines

Outline

Introduction: End-point singularity

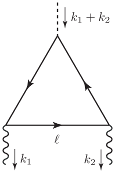

Figure: $H \to b\bar{b} \to \gamma\gamma$ at leading order.

- Large logarithms $\ln(\frac{m_H^2}{m_b^2})$: need resummation
- Traditional light-cone approach leads to end-point divergence $\int_0^1 \frac{1}{z}$, when ℓ becomes soft, $z \to 0$ (z is the fraction of collinear momentum carried by ℓ)
- Generally appears in next-to-leading power corrections

Introduction: Factorization using SCET

Factorization using SCET (Z. L. Liu and M. Neubert, JHEP **04**, 033 (2020) and series of papers):

$$\mathcal{M}_b(H \to \gamma\gamma) = \sum_{i=1}^{3} H_i \langle \gamma\gamma | \mathcal{O}_i | H \rangle, \tag{1}$$

Soft sector (end-point singularities are involved):

$$\begin{aligned} \mathcal{O}_3 \; &= H(0) \int d^D x \int d^D y \, T\Big\{ \Big[\Big(\mathcal{A}_{n_1}^{\perp}(x) + \mathcal{G}_{n_1}^{\perp}(x) \Big) \mathcal{X}_{n_1}(x) \Big]^{\alpha i} \bar{\mathcal{X}}_{n_1}^{\beta j}(0) \Big\} \\ &\times T\Big\{ \mathcal{X}_{n_2}^{\beta k}(0) \Big[\bar{\mathcal{X}}_{n_2}(y) \Big(\mathcal{A}_{n_2}^{\perp}(y) + \mathcal{G}_{n_2}^{\perp}(y) \Big) \Big]^{\gamma l} \Big\} \\ &\times T\Big\{ \Big[S_{n_2}^{\dagger}(y_+) q_s(y_+) \Big]^{\gamma l} [\bar{q}_s(x_-) S_{n_1}(x_-)]^{\alpha i} \Big[S_{n_1}^{\dagger}(0) S_{n_2}(0) \Big]^{jk} \Big\} + \text{h.c.}, \end{aligned} \tag{2}$$

Factorize into convolution of jet functions and soft-quark function ($\omega = \ell_+ \ell_-$):

$$\langle \gamma\gamma | \mathcal{O}_3 | H \rangle = 2 g_{\perp}^{\mu\nu} \int_0^{\infty} \frac{d\omega}{\omega} S_1(\omega) \int_{\sqrt{\omega}}^{\infty} \frac{d\ell_-}{\ell_-} J(m_H \omega / \ell_-) J(-m_H \ell_-). \tag{3}$$

Outline

Definition of soft function

Soft function:

$$\boldsymbol{S}(\ell_+,\ell_-) = \frac{i\pi}{N_c}\int dx_-\,dy_+\,\exp\left[i\frac{\ell_- y_+ - \ell_+ x_-}{2}\right]$$
$$\times\langle 0|\,T\,\mathrm{Tr}\left[S_{n_2}(0)S^\dagger_{n_2}(y_+,0,\mathbf{0}_\perp)q_s(y_+,0,\mathbf{0}_\perp)\bar{q}_s(0,x_-,\mathbf{0}_\perp)S_{n_1}(0,x_-,\mathbf{0}_\perp)S^\dagger_{n_1}(0)\right]|0\rangle. \quad (4)$$

The momenta flow into the positions x_- and y_+ are fixed by ℓ_+ and ℓ_- respectively, which is required to factorize the two jet functions from the soft-quark function.

It is much easier to do renormalization before integrating $\ell_\perp$ and extracting discontinuity, which does not introduce extra divergences. So we define the un-integrated soft-function:

$$\begin{aligned}\boldsymbol{S}(\ell_+,\ell_-,\ell_\perp) &= \frac{i\pi}{N_c}\int dx_-\,dy_+\,d^{D-2}\boldsymbol{z}_\perp\,\exp\left[i\left(\frac{\ell_- y_+ - \ell_+ x_-}{2} - \boldsymbol{\ell}_\perp\cdot\boldsymbol{z}_\perp\right)\right]\\ &\quad\times\langle 0|\,T\,\mathrm{Tr}\Big[S_{n_2}(0,0,\boldsymbol{z}_\perp/2)S^\dagger_{n_2}(y_+,0,\boldsymbol{z}_\perp/2)q_s(y_+,0,\boldsymbol{z}_\perp/2)\\ &\quad\times\bar{q}_s(0,x_-,-\boldsymbol{z}_\perp/2)S_{n_1}(0,x_-,-\boldsymbol{z}_\perp/2)S^\dagger_{n_1}(0,0,-\boldsymbol{z}_\perp/2)\Big]|0\rangle. \quad (5)\end{aligned}$$

Structure functions and discontinuities

Due to reparameterization invariance, we can decompose the un-integrated soft function into 8 independent structure functions

$$\begin{aligned} \boldsymbol{S}(\ell_+,\ell_-,\ell_\perp) = {} & m_b \boldsymbol{S}_1(\omega,\boldsymbol{\ell}_\perp^2) + \frac{\not{n}_1}{2}(n_2\cdot\ell)\boldsymbol{S}_2(\omega,\boldsymbol{\ell}_\perp^2) + \frac{\not{n}_2}{2}(n_1\cdot\ell)\boldsymbol{S}_3(\omega,\boldsymbol{\ell}_\perp^2) \\ & + m_b\frac{\not{n}_2\not{n}_1}{4}\boldsymbol{S}_4(\omega,\boldsymbol{\ell}_\perp^2) + \not{\boldsymbol{\ell}}_\perp \boldsymbol{S}_5(\omega,\boldsymbol{\ell}_\perp^2) + \frac{m_b\not{n}_1\not{\boldsymbol{\ell}}_\perp}{2(n_1\cdot\ell)}\boldsymbol{S}_6(\omega,\boldsymbol{\ell}_\perp^2) \\ & + \frac{m_b\not{\boldsymbol{\ell}}_\perp\not{n}_2}{2(n_2\cdot\ell)}\boldsymbol{S}_7(\omega,\boldsymbol{\ell}_\perp^2) + \frac{\not{n}_2\not{\boldsymbol{\ell}}_\perp\not{n}_1}{4}\boldsymbol{S}_8(\omega,\boldsymbol{\ell}_\perp^2). \end{aligned} \tag{6}$$

Decomposition of soft function into structure functions

$$\boldsymbol{S}(\ell_+,\ell_-) = m_b\boldsymbol{S}_1(\omega) + \frac{\not{n}_1}{2}(n_2\cdot\ell)\boldsymbol{S}_2(\omega) + \frac{\not{n}_2}{2}(n_1\cdot\ell)\boldsymbol{S}_3(\omega) + m_b\frac{\not{n}_2\not{n}_1}{4}\boldsymbol{S}_4(\omega). \tag{7}$$

Discontinuity of the soft function

$$S_i(\omega) = \frac{1}{2\pi i}[\boldsymbol{S}_i(\omega+i\varepsilon) - \boldsymbol{S}_i(\omega-i\varepsilon)]. \tag{8}$$

Leading-order soft function and discontinuities

Leading-order soft function

$$\boldsymbol{S}^{\mathsf{LO}}(\ell_+,\ell_-) = m_b \boldsymbol{S}_1^{\mathsf{LO}}(\omega) + \frac{\not{n}_1}{2}\, n_2\cdot\ell\, \boldsymbol{S}_2^{\mathsf{LO}}(\omega) + \frac{\not{n}_2}{2}\, n_1\cdot\ell\, \boldsymbol{S}_3^{\mathsf{LO}}(\omega), \tag{9}$$

where the LO structure functions are (ϵ poles come from $\ell_\perp$ integration)

$$\boldsymbol{S}_{1,2,3}^{\mathsf{LO}}(\omega) = (4\pi)^\epsilon \Gamma(\epsilon) \left(-\omega + m_b^2 - i\varepsilon\right)^{-\epsilon}. \tag{10}$$

The discontinuities of the LO soft structure functions are

$$S_{1,2,3}^{\mathsf{LO}}(\omega) = \frac{(4\pi)^\epsilon}{\Gamma(1-\epsilon)} \left(\omega - m_b^2\right)^{-\epsilon} \theta(\omega - m_b^2) = \theta(\omega - m_b^2)\left[1 + O(\epsilon)\right], \tag{11}$$

from which we can see the discontinuities of the LO soft function has no ϵ pole from the $\ell_\perp$ integration.

Outline

Light-front perturbation theory

We need to know the analyticity of the soft function in order to work out the factorization form. Also we use it to compute the renormalization of the soft function.

In light-front perturbation theory, imaginary contributions arise from vanishing energy denominators.

Feynman rules in light-front perturbation theory:

- (i) vertices, whose Feynman rules are the same as in covariant perturbation theory,
- (ii) energy denominators for each intermediate state, which consist of the incoming light-front energy minus the on-shell light-front energies of the particles that are included in the intermediate state,
- (iii) factors of the inverse of the longitudinal ($+$) momenta of the intermediate-state particles (this is the relativistic normalization of the states in light-front perturbation theory),
- (iv) integrations over the $+$ and transverse components of the loop momenta.

For each intermediate-state line, the $+$-light-front longitudinal component of momentum is always positive.

Example

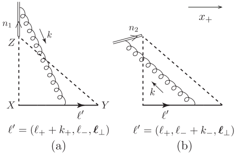

For diagram (a), the propagator denominators are (starting from covariant Feynman rules)

$$\frac{1}{-k_+ + i\varepsilon}\,\frac{1}{k^2 + i\varepsilon}\,\frac{1}{(\ell_+ + k_+)\ell_- - \boldsymbol{\ell}_\perp^2 - m_b^2 + i\varepsilon} \times \frac{1}{\ell_+(\ell_- - k_-) - (\boldsymbol{\ell}_\perp - \boldsymbol{k}_\perp)^2 - m_b^2 + i\varepsilon}. \tag{12}$$

Assuming $\ell_+ > 0$, completing the k_- contour integration gives

$$-2\pi i\theta(k_+)\frac{1}{\ell_+}\,\frac{1}{\ell_+ + k_+}\,\frac{1}{k_+}\,\frac{1}{-k_+ + i\varepsilon}\,\frac{1}{\ell_- - \boldsymbol{k}_\perp^2/k_+ - [(\boldsymbol{\ell}_\perp - \boldsymbol{k}_\perp)^2 + m_b^2]/\ell_+ + i\varepsilon} \times \frac{1}{\ell_- - (\boldsymbol{\ell}_\perp^2 + m_b^2)/(\ell_+ + k_+) + i\varepsilon}. \tag{13}$$

Conclusion about the analyticity of the soft function

For diagram (b), a light-front analysis of the denominators gives (or by completing k_- contour integration from covariant perturbative theory)

$$-2\pi i\theta(-k_+)\frac{1}{\ell_+}\frac{1}{k_+}\frac{1}{\ell_+ - k_+}\frac{1}{\boldsymbol{k}_\perp^2/k_+}\frac{1}{\ell_- + \boldsymbol{k}_\perp^2/k_+ - (\boldsymbol{\ell}_\perp^2 + m_b^2)/\ell_+ + i\varepsilon}$$
$$\times\frac{1}{\ell_- - [(\boldsymbol{\ell}_\perp - \boldsymbol{k}_\perp)^2 + m_b^2]/(\ell_+ - k_+) + i\varepsilon}. \qquad (14)$$

Owing to the unorthodox momentum routing in the soft function, a soft-quark line can carry an infinite $+$ longitudinal momentum without causing any particle line to move backward.

In addition, due to the positivity of the light-front energies (no backward-moving particles), the energy denominators will never vanish when $\ell_- < 0$ (ie: $\omega < 0$).

Conclusion: The soft function is analytic everywhere in the complex ω plane except for the cut along the positive real axis.

Outline

Difficulties in renormalization of the soft function

The α_s-order soft function is given by Z. L. Liu and M. Neubert, JHEP **04**, 033 (2020), from which one can extract the UV divergences:

$$S^{\mathrm{UV}} = \frac{\alpha_s C_F}{4\pi}\left\{ \left(\frac{\omega - m_b^2}{\mu^2}\right)^{-2\epsilon}\left[-\frac{2}{\epsilon^2} + \frac{6}{\epsilon} + \frac{2}{\epsilon}\log\left(\frac{\omega - m_b^2}{\omega}\right)\right]\theta(\omega - m_b^2) - \frac{4}{\epsilon}\log\left(\frac{m_b^2 - \omega}{m_b^2}\right)\theta(m_b^2 - \omega)\right\}. \tag{15}$$

However, the conjectured renormalization factor Z_S given in Z. L. Liu, B. Mecaj, M. Neubert, X. Wang and S. Fleming, JHEP **07**, 104 (2020) is

$$Z_S = \delta(\omega' - \omega) + \frac{\alpha_s C_F}{4\pi}\frac{1}{\epsilon}\left\{\left[\frac{2}{\epsilon} + 2\log\left(\frac{\mu^2}{\omega}\right) - 3\right]\delta(\omega' - \omega) - 4\omega\left[\frac{\theta(\omega' - \omega)}{\omega'(\omega' - \omega)} + \frac{\theta(\omega - \omega')}{\omega(\omega - \omega')}\right]_+\right\}. \tag{16}$$

- The unorthodox momentum routing in the soft function leads to nonlocal contributions in the renormalization
- Explicit fix-order calculation loses the non-local information of the soft function

Renormalization formula

Renormalization of the soft operator $\mathcal{O}_S(\ell_+, \ell_-)$:

$$\mathcal{O}_S^R(\ell_+, \ell_-) = \frac{1}{2} \int d\ell'_+ \, d\ell'_- \, Z_S(\ell_+, \ell_-, \ell'_+, \ell'_-; \mu^2) \mathcal{O}_S(\ell'_+, \ell'_-), \tag{17}$$

$$Z_S = Z_S^{(0)} + \alpha_s Z_S^{(1)} + \alpha_s^2 Z_S^{(2)} + \cdots . \tag{18}$$

In terms of vacuum-to-vacuum matrix element, at one-loop order

$$\boldsymbol{S}_{(i)}(\ell_+, \ell_-) = \frac{1}{2} \int d\ell'_+ \, d\ell'_- \, c_{(i)}(\ell_+, \ell_-, \ell'_+, \ell'_-; \mu^2) \boldsymbol{S}(\ell'_+, \ell'_-), \tag{19}$$

where $\boldsymbol{S}(\ell'_+, \ell'_-)$ is the all-order soft function with shifted arguments.

Diagrammatic form of $\boldsymbol{S}(\ell_+, \ell_-)$

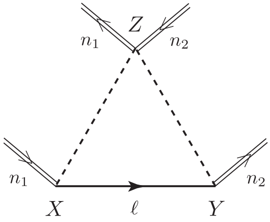

Figure: The solid line is a soft-quark propagator. The double solid lines with incoming arrows are Wilson lines S_{n_i}, and the double solid lines with outgoing arrows are hermitian-conjugate Wilson lines $S^\dagger_{n_i}$. The dashed lines indicate a space-time separation (space-time separations of the jet functions). A jet in the $\pm$ light-front direction is insensitive to external momenta in the $\pm$ or $\perp$ directions, which allows factorization of the Wilson lines of the soft function from the jet functions.

Feynman rules for Wilson line

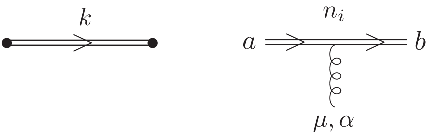

$$\frac{i}{k \cdot n_i + i\varepsilon} \qquad\qquad i g_s n_i^{\mu} (T^{\alpha})_{ba}$$

(a) (b)

Figure: Feynman rules for a Wilson line S_{n_i} that is collinear to n_i. (a) The Wilson-line propagator. (b) The vertex for the interaction of a gluon with the Wilson line.

Diagram A

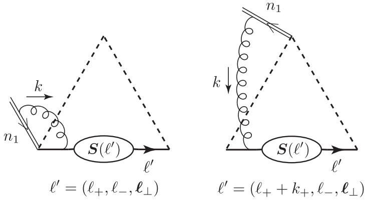

The non-local terms come from diagram (b).

$$\boldsymbol{S}_{(A)}(\ell_+, \ell_-) = i g_s^2 C_F \left(\frac{\mu^2 e^{\gamma_E}}{4\pi} \right)^\epsilon \int_{\boldsymbol{\ell}_\perp} \int \frac{dk_+ dk_- d^{D-2} k_\perp}{(2\pi)^D} \frac{1}{(-k_+ + i\varepsilon)(k^2 + i\varepsilon)}$$
$$\times \left\{ - \frac{\boldsymbol{S}(\ell_+, \ell_-, \ell_\perp) \frac{\not{n}_1}{2} \left[\frac{\not{n}_2}{2} (\ell_+ - k_+) + \not{\ell}_\perp - \not{k}_\perp + m_b \right]}{(\ell_+ - k_+)(\ell_- - k_-) - (\boldsymbol{\ell}_\perp - \boldsymbol{k}_\perp)^2 - m_b^2 + i\varepsilon} + \frac{\boldsymbol{S}(\ell_+ + k_+, \ell_-, \ell_\perp) \frac{\not{n}_1}{2} (\frac{\not{n}_2}{2} \ell_+ + \not{\ell}_\perp - \not{k}_\perp + m_b)}{\ell_+(\ell_- - k_-) - (\boldsymbol{\ell}_\perp - \boldsymbol{k}_\perp)^2 - m_b^2 + i\varepsilon} \right\}. \quad (20)$$

k_- contour integration

Assuming $\ell_+ > 0$, $\ell_- < 0$ and completing the k_- contour integration by picking up the pole $k_- = \frac{k_\perp^2}{k_+} - i\varepsilon$

$$\boldsymbol{S}_{(A)}(\ell_+,\ell_-) = -2\alpha_s C_F \left(\frac{\mu^2 e^{\gamma_E}}{4\pi}\right)^{\epsilon} \int_{\boldsymbol{\ell}_\perp} \int \frac{d^{D-2}k_\perp}{(2\pi)^{D-2}} \int_0^\infty \frac{dk_+}{k_+^2}$$
$$\times \left\{ -\frac{\theta(\ell_+ - k_+)\boldsymbol{S}(\ell_+,\ell_-)\frac{\not{n}_1}{2}\left[\frac{\not{n}_2}{2}(\ell_+ - k_+) + \not{\ell}_\perp - \not{k}_\perp + m_b\right]}{(\ell_+ - k_+)\ell_- - \frac{\ell_+ - k_+}{k_+}\boldsymbol{k}_\perp^2 - (\boldsymbol{\ell}_\perp - \boldsymbol{k}_\perp)^2 - m_b^2 + i\varepsilon} \right.$$
$$\left. + \frac{\boldsymbol{S}(\ell_+ + k_+, \ell_-, \ell_\perp)\frac{\not{n}_1}{2}(\frac{\not{n}_2}{2}\ell_+ + \not{\ell}_\perp - \not{k}_\perp + m_b)}{\ell_+\ell_- - \frac{\ell_+}{k_+}\boldsymbol{k}_\perp^2 - (\boldsymbol{\ell}_\perp - \boldsymbol{k}_\perp)^2 - m_b^2 + i\varepsilon} \right\}. \qquad (21)$$

Extract UV divergences

After shifting $k_\perp$

$$\boldsymbol{S}_{(A)}(\ell_+,\ell_-) = 2\alpha_s C_F \left(\frac{\mu^2 e^{\gamma_E}}{4\pi}\right)^{\epsilon} \int_{\boldsymbol{\ell}_\perp} \int \frac{d^{D-2}k_\perp}{(2\pi)^{D-2}} \int_0^\infty \frac{dk_+}{k_+}$$
$$\times \left\{ -\frac{\theta(\ell_+-k_+)}{\ell_+} \frac{\boldsymbol{S}(\ell_+,\ell_-)\frac{\not{n}_1}{2}\left[\frac{\not{n}_2}{2}(\ell_+-k_+) + \not{\ell}_\perp \frac{\ell_+-k_+}{\ell_+} + m_b\right]}{\boldsymbol{k}_\perp^2 - \frac{k_+}{\ell_+}\left(\ell^2 - m_b^2 - \ell_- k_+ + \frac{k_+}{\ell_+}\boldsymbol{\ell}_\perp^2\right) - i\varepsilon} \right.$$
$$\left. + \frac{1}{\ell_+ + k_+} \frac{\boldsymbol{S}(\ell_+ + k_+,\ell_-)\frac{\not{n}_1}{2}\left(\frac{\not{n}_2}{2}\ell_+ + \not{\ell}_\perp \frac{\ell_+}{\ell_+ + k_+} + m_b\right)}{\boldsymbol{k}_\perp^2 - \frac{k_+\ell_+(\ell^2-m_b^2)+k_+^2(\ell_+\ell_- - m_b^2)}{(\ell_+ + k_+)^2} - i\varepsilon} \right\}. \quad (22)$$

Extract the UV divergences

$$\boldsymbol{S}^{\mathsf{UV}}_{(A)}(\ell_+,\ell_-) = \frac{\alpha_s C_F}{2\pi}\frac{1}{\epsilon_{\mathsf{UV}}} \int_{\boldsymbol{\ell}_\perp} \int_0^\infty \frac{dk_+}{k_+}$$
$$\times \left\{ -\boldsymbol{S}(\ell_+,\ell_-,\ell_\perp)\frac{\not{n}_1}{2} \frac{\theta(\ell_+-k_+)\left[\frac{\not{n}_2}{2}(\ell_+-k_+) + \not{\ell}_\perp \frac{\ell_+-k_+}{\ell_+} + m_b\right]}{\ell_+} \right.$$
$$\left. + \boldsymbol{S}(\ell_+ + k_+,\ell_-,\ell_\perp)\frac{\not{n}_1}{2} \frac{\left(\frac{\not{n}_2}{2}\ell_+ + \not{\ell}_\perp \frac{\ell_+}{\ell_+ + k_+} + m_b\right)}{\ell_+ + k_+} \right\}. \quad (23)$$

UV divergence of diagram A

The change of variables $k_+ = x\ell_+$ leads to

$$\boldsymbol{S}^{\mathsf{UV}}_{(A)}(\ell_+,\ell_-) = \frac{\alpha_s C_F}{2\pi}\frac{1}{\epsilon_{\mathsf{UV}}}\int_{\boldsymbol{\ell}_\perp}\Bigg\{\boldsymbol{S}(\ell_+,\ell_-,\ell_\perp)\frac{\not{n}_1}{2}\left(\frac{\not{n}_2}{2}+\frac{\not{\ell}_\perp}{\ell_+}\right)$$
$$+\int_0^\infty dx\Bigg[\frac{\boldsymbol{S}(\ell_+(1+x),\ell_-,\ell_\perp)}{x(1+x)}\frac{\not{n}_1}{2}\left(\frac{\not{n}_2}{2}+\frac{\not{\ell}_\perp}{\ell_+}\frac{1}{1+x}+\frac{m_b}{\ell_+}\right)$$
$$-\frac{\theta(1-x)\boldsymbol{S}(\ell_+,\ell_-,\ell_\perp)}{x}\frac{\not{n}_1}{2}\left(\frac{\not{n}_2}{2}+\frac{\not{\ell}_\perp}{\ell_+}+\frac{m_b}{\ell_+}\right)\Bigg]\Bigg\}. \quad (24)$$

Transformations $\frac{x}{1-x}\to u\to x$ for $\boldsymbol{S}(\ell_+,\ell_-,\ell_\perp)$ terms

$$\boldsymbol{S}^{\mathsf{UV}}_{(A)}(\ell_+,\ell_-)$$
$$=\frac{\alpha_s C_F}{2\pi}\frac{1}{\epsilon_{\mathsf{UV}}}\int_{\boldsymbol{\ell}_\perp}\Bigg[\boldsymbol{S}(\ell_+,\ell_-,\ell_\perp)\left(1-\frac{\not{n}_2\not{n}_1}{4}+\frac{n_2\cdot\ell}{\omega}\frac{\not{n}_1\not{\ell}_\perp}{2}\right)$$
$$+\int_0^\infty dx\Bigg\{\frac{\boldsymbol{S}(\ell_+(1+x),\ell_-,\ell_\perp)}{x(1+x)}\left[1-\frac{\not{n}_2\not{n}_1}{4}+\frac{n_2\cdot\ell}{(1+x)\omega}\frac{\not{n}_1\not{\ell}_\perp}{2}+\frac{m_b(n_2\cdot\ell)}{\omega}\frac{\not{n}_1}{2}\right]$$
$$-\frac{\boldsymbol{S}(\ell_+,\ell_-,\ell_\perp)}{x(1+x)}\left[1-\frac{\not{n}_2\not{n}_1}{4}+\frac{n_2\cdot\ell}{\omega}\frac{\not{n}_1\not{\ell}_\perp}{2}+\frac{m_b(n_2\cdot\ell)}{\omega}\frac{\not{n}_1}{2}\right]\Bigg\}\Bigg]. \quad (25)$$

UV divergence of diagram A′

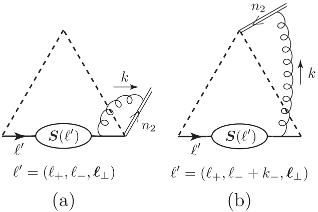

The non-local terms come from diagram (b).

$$\begin{aligned} & \boldsymbol{S}^{\text{UV}}_{(A')}(\ell_+,\ell_-) \\ = & \frac{\alpha_s C_F}{2\pi}\frac{1}{\epsilon_{\text{UV}}}\int_{\boldsymbol{\ell}_\perp}\Bigg[\left(1-\frac{\not{n}_2\not{n}_1}{4}+\frac{n_1\cdot\ell}{\omega}\frac{\not{\ell}_\perp\not{n}_2}{2}\right)\boldsymbol{S}(\ell_+,\ell_-,\ell_\perp) \\ & +\int_0^\infty dx\Bigg\{\left[1-\frac{\not{n}_2\not{n}_1}{4}+\frac{n_1\cdot\ell}{(1+x)\omega}\frac{\not{\ell}_\perp\not{n}_2}{2}+\frac{m_b(n_1\cdot\ell)}{\omega}\frac{\not{n}_2}{2}\right]\frac{\boldsymbol{S}(\ell_+,(1+x)\ell_-,\ell_\perp)}{x(1+x)} \\ & -\left[1-\frac{\not{n}_2\not{n}_1}{4}+\frac{n_1\cdot\ell}{\omega}\frac{\not{\ell}_\perp\not{n}_2}{2}+\frac{m_b(n_1\cdot\ell)}{\omega}\frac{\not{n}_2}{2}\right]\frac{\boldsymbol{S}(\ell_+,\ell_-,\ell_\perp)}{x(1+x)}\Bigg\}\Bigg]. \end{aligned} \tag{26}$$

Diagram B

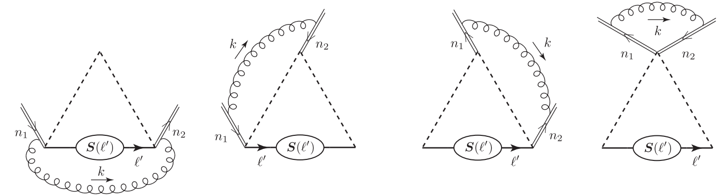

$\ell' = (\ell_+ - k_+, \ell_- - k_-, \boldsymbol{\ell}_\perp)$ (a) $\quad$ $\ell' = (\ell_+ - k_+, \ell_-, \boldsymbol{\ell}_\perp)$ (b) $\quad$ $\ell' = (\ell_+, \ell_- - k_-, \boldsymbol{\ell}_\perp)$ (c) $\quad$ $\ell' = (\ell_+, \ell_-, \boldsymbol{\ell}_\perp)$ (d)

The non-local terms come from diagram (a, b, c).

$$\boldsymbol{S}_{(B)}(\ell_+, \ell_-) = i g_s^2 C_F \left(\frac{\mu^2 e^{\gamma_E}}{4\pi}\right)^{\epsilon} \int \frac{dk_+ \, dk_- \, d^{D-2} k_\perp}{(2\pi)^D} \frac{1}{(-k_+ + i\varepsilon)(k_- + i\varepsilon)(k^2 + i\varepsilon)} \times \Big[\boldsymbol{S}(\ell_+ - k_+, \ell_- - k_-) - \boldsymbol{S}(\ell_+ - k_+, \ell_-) - \boldsymbol{S}(\ell_+, \ell_- - k_-) + \boldsymbol{S}(\ell_+, \ell_-)\Big]. \quad (27)$$

k_- contour integration

Completing k_- contour integration gives

$$\boldsymbol{S}_{(B)}(\ell_+,\ell_-) = -2\alpha_s C_F \left(\frac{\mu^2 e^{\gamma_E}}{4\pi}\right)^\epsilon \int_{-\infty}^{0} \frac{dk_+}{(-k_+)} \int \frac{d^{D-2}k_\perp}{(2\pi)^{D-2}} \frac{1}{\boldsymbol{k}_\perp^2}$$
$$\times \Bigg[\theta(\ell_+ - k_+)\boldsymbol{S}(\ell_+ - k_+, \ell_-) + \theta(k_+ - \ell_+)\boldsymbol{S}(\ell_+ - k_+, \ell_- - \tfrac{\boldsymbol{k}_\perp^2}{k_+})$$
$$-\boldsymbol{S}(\ell_+ - k_+, \ell_-) - \boldsymbol{S}(\ell_+, \ell_- - \tfrac{\boldsymbol{k}_\perp^2}{k_+}) + \boldsymbol{S}(\ell_+, \ell_-)\Bigg]. \quad (28)$$

Making the change of variables $\boldsymbol{k}_\perp^2 = x k_+ \ell_-$ and splitting the k_+ integration region $[-\infty, 0]$ into $[-\infty, \ell_+]$ and $[\ell_+, 0]$, we obtain

$$\boldsymbol{S}_{(B)}(\ell_+,\ell_-) = \frac{\alpha_s C_F}{2\pi} \frac{(\mu^2 e^{\gamma_E})^\epsilon}{\Gamma(1-\epsilon)} (\ell_-)^{-\epsilon} \int_{-\infty}^{0} dx \frac{1}{(-x)^{1+\epsilon}}$$
$$\times \Bigg\{ \int_{\ell_+}^{0} \frac{dk_+}{(-k_+)^{1+\epsilon}} \Big[\boldsymbol{S}(\ell_+ - k_+, \ell_-) - \boldsymbol{S}(\ell_+ - k_+, \ell_-(1-x))$$
$$+\boldsymbol{S}(\ell_+, \ell_-(1-x)) - \boldsymbol{S}(\ell_+, \ell_-)\Big]$$
$$+ \int_{-\infty}^{\ell_+} \frac{dk_+}{(-k_+)^{1+\epsilon}} \Big[\boldsymbol{S}(\ell_+, \ell_-(1-x)) - \boldsymbol{S}(\ell_+, \ell_-)\Big] \Bigg\}. \quad (29)$$

UV divergence of diagram B

For the finite k_+ integral, set $k_+ = x\ell_+$:

$$\begin{aligned}
&\boldsymbol{S}^{\mathsf{UV}}_{(B)}(\ell_+,\ell_-) \\
&= \frac{\alpha_s C_F}{2\pi}\frac{1}{\epsilon_{\mathsf{UV}}}\Bigg\{-\left[\frac{1}{\epsilon_{\mathsf{UV}}}+\log\left(\frac{\mu^2}{-\omega-i\varepsilon}\right)\right]\boldsymbol{S}(\ell_+,\ell_-)-\int_{-\infty}^{-1}dx\frac{\boldsymbol{S}(\ell_+,\ell_-(1-x))}{x} \\
&\quad+\int_0^1 dx\frac{\boldsymbol{S}(\ell_+(1-x),\ell_-)-\boldsymbol{S}(\ell_+,\ell_-)}{x}-\int_{-1}^{0}dx\frac{\boldsymbol{S}(\ell_+,\ell_-(1-x))-\boldsymbol{S}(\ell_+,\ell_-)}{x}\Bigg\}.
\end{aligned} \tag{30}$$

We re-write the negative x integration as

$$\begin{aligned}
&-\int_{-\infty}^{-1}\frac{dx}{x}\boldsymbol{S}(\ell_+,\ell_-(1-x))-\int_{-1}^{0}\frac{dx}{x}\left[\boldsymbol{S}(\ell_+,\ell_-(1-x))-\boldsymbol{S}(\ell_+,\ell_-)\right] \\
&=\lim_{\delta\to 0}\left[-\int_{-\infty}^{-\delta}\frac{dx}{x}\boldsymbol{S}(\ell_+,\ell_-(1-x))-\int_{-1}^{-\delta}\frac{dx}{x}\boldsymbol{S}(\ell_+,\ell_-)\right]
\end{aligned} \tag{31}$$

The contribution of the semicircle at infinity vanishes, and the contribution of the small semicircle is $\pm i\pi S(\omega)$. Then we split the integration region $[0,+\infty]$ into $[0,1]$ and $[1,+\infty]$.

UV divergences of diagram B and C

UV divergence of diagram B

$$\boldsymbol{S}^{\mathsf{UV}}_{(B)}(\ell_+,\ell_-) = \frac{\alpha_s C_F}{2\pi}\frac{1}{\epsilon_{\mathsf{UV}}}\Bigg\{-\left[\frac{1}{\epsilon_{\mathsf{UV}}}+\log\left(\frac{\mu^2}{\omega+i\varepsilon}\right)\right]\boldsymbol{S}(\ell_+,\ell_-) + \int_0^1 dx\frac{\boldsymbol{S}(\ell_+(1-x),\ell_-)+\boldsymbol{S}(\ell_+,\ell_-(1-x))-2\boldsymbol{S}(\ell_+,\ell_-)}{x} + \int_1^\infty dx\frac{\boldsymbol{S}(\ell_+,\ell_-(1-x))}{x}\Bigg\}. \tag{32}$$

UV divergence of the soft quark self-energy diagram (after renormalization of quark mass):

$$\boldsymbol{S}^{\mathsf{UV}}_{(C)}(\ell_+,\ell_-) = -\frac{\alpha_s C_F}{4\pi}\frac{1}{\epsilon_{\mathsf{UV}}}\boldsymbol{S}(\ell_+,\ell_-), \tag{33}$$

which is the soft-quark wave-function renormalization.

Total UV divergence at α_s order

$$\begin{aligned}
\boldsymbol{S}^{\mathrm{UV}}(\ell_+,\ell_-) &= \boldsymbol{S}^{\mathrm{UV}}_{(A)}(\ell_+,\ell_-) + \boldsymbol{S}^{\mathrm{UV}}_{(A')}(\ell_+,\ell_-) + \boldsymbol{S}^{\mathrm{UV}}_{(B)}(\ell_+,\ell_-) + \boldsymbol{S}^{\mathrm{UV}}_{(C)}(\ell_+,\ell_-) \\
&= \frac{\alpha_s C_F}{2\pi}\frac{1}{\epsilon_{\mathrm{UV}}}\int_{\boldsymbol{\ell}_\perp}\Bigg[\boldsymbol{S}(\ell_+,\ell_-,\ell_\perp)\left(1-\frac{\not{n}_2\not{n}_1}{4}+\frac{n_2\cdot\ell}{\omega}\frac{\not{n}_1\not{\ell}_\perp}{2}\right) \\
&\quad + \int_0^\infty dx\Bigg\{\frac{\boldsymbol{S}(\ell_+(1+x),\ell_-,\ell_\perp)}{x(1+x)}\left[1-\frac{\not{n}_2\not{n}_1}{4}+\frac{n_2\cdot\ell}{(1+x)\omega}\frac{\not{n}_1\not{\ell}_\perp}{2}+\frac{m_b(n_2\cdot\ell)}{\omega}\frac{\not{n}_1}{2}\right] \\
&\quad - \frac{\boldsymbol{S}(\ell_+,\ell_-,\ell_\perp)}{x(1+x)}\left[1-\frac{\not{n}_2\not{n}_1}{4}+\frac{n_2\cdot\ell}{\omega}\frac{\not{n}_1\not{\ell}_\perp}{2}+\frac{m_b(n_2\cdot\ell)}{\omega}\frac{\not{n}_1}{2}\right]\Bigg\}\Bigg] \\
&\quad + \frac{\alpha_s C_F}{2\pi}\frac{1}{\epsilon_{\mathrm{UV}}}\int_{\boldsymbol{\ell}_\perp}\Bigg[\left(1-\frac{\not{n}_2\not{n}_1}{4}+\frac{n_1\cdot\ell}{\omega}\frac{\not{\ell}_\perp\not{n}_2}{2}\right)\boldsymbol{S}(\ell_+,\ell_-,\ell_\perp) \\
&\quad + \int_0^\infty dx\Bigg\{\left[1-\frac{\not{n}_2\not{n}_1}{4}+\frac{n_1\cdot\ell}{(1+x)\omega}\frac{\not{\ell}_\perp\not{n}_2}{2}+\frac{m_b(n_1\cdot\ell)}{\omega}\frac{\not{n}_2}{2}\right]\frac{\boldsymbol{S}(\ell_+,(1+x)\ell_-,\ell_\perp)}{x(1+x)} \\
&\quad - \left[1-\frac{\not{n}_2\not{n}_1}{4}+\frac{n_1\cdot\ell}{\omega}\frac{\not{\ell}_\perp\not{n}_2}{2}+\frac{m_b(n_1\cdot\ell)}{\omega}\frac{\not{n}_2}{2}\right]\frac{\boldsymbol{S}(\ell_+,\ell_-,\ell_\perp)}{x(1+x)}\Bigg\}\Bigg] \\
&\quad + \frac{\alpha_s C_F}{2\pi}\frac{1}{\epsilon_{\mathrm{UV}}}\Bigg\{-\left[\frac{1}{\epsilon_{\mathrm{UV}}}+\log\left(\frac{\mu^2}{\omega}\right)\right]\boldsymbol{S}(\ell_+,\ell_-)+\int_1^\infty dx\frac{\boldsymbol{S}(\ell_+,\ell_-(1-x))}{x} \\
&\quad + \int_0^1 dx\frac{\boldsymbol{S}(\ell_+(1-x),\ell_-)+\boldsymbol{S}(\ell_+,\ell_-(1-x))-2\boldsymbol{S}(\ell_+,\ell_-)}{x}\Bigg\} \\
&\quad - \frac{\alpha_s C_F}{4\pi}\frac{1}{\epsilon_{\mathrm{UV}}}\int_{\boldsymbol{\ell}_\perp}\boldsymbol{S}(\ell_+,\ell_-,\ell_\perp). \qquad (34)
\end{aligned}$$

Z_S at α_s order

Define several additional structure functions

$$\boldsymbol{S}_i(\omega) = \int_{\boldsymbol{\ell}_\perp} \boldsymbol{S}_i(\omega, \boldsymbol{\ell}_\perp^2) \frac{\boldsymbol{\ell}_\perp^2}{\omega}, \quad \text{for } i = 5,\ 6,\ 7, \text{ and } 8. \tag{35}$$

Make the following changes of integration variables: $\omega' = (1+x)\omega$ for $\boldsymbol{S}_{(A)}^{\mathrm{UV}}$ and $\boldsymbol{S}_{(A')}^{\mathrm{UV}}$, and $\omega' = (1-x)\omega$ for $\boldsymbol{S}_{(B)}^{\mathrm{UV}}$, then the renormalized structure functions can be expressed as

$$S_i^{\mathrm{R}}(\omega) = \sum_{j=1}^{8} \int_0^\infty d\omega'\, Z_S^{ij}(\omega, \omega'; \mu) S_j(\omega'), \quad \text{for } i = 1,\ 2,\ 3, \text{ and } 4, \tag{36}$$

where

$$Z_S^{ij}(\omega, \omega'; \mu) = \delta(\omega - \omega')\delta^{ij} + \frac{\alpha_s C_F}{4\pi} \frac{1}{\epsilon_{\mathrm{UV}}} \boldsymbol{M}_S^{ij}(\omega, \omega'; \mu), \tag{37}$$

$M_S^{ij}(\omega, \omega'; \mu)$

$$
\begin{aligned}
&M_S(\omega, \omega'; \mu) \\
&= \begin{pmatrix}
d - 2a - 2b - 2c & 0 & 0 & 0 & 0 & 0 & 0 & 0 \\
-\frac{m_b^2}{\omega} b & d - a - \frac{\omega'}{\omega} b - \frac{\omega' + \omega}{\omega} c & 0 & 0 & -(a+b) & 0 & 0 & 0 \\
-\frac{m_b^2}{\omega} b & 0 & d - a - \frac{\omega'}{\omega} b - \frac{\omega' + \omega}{\omega} c & 0 & -(a+b) & 0 & 0 & 0 \\
2(a+b) & -\frac{\omega'}{\omega} b & -\frac{\omega'}{\omega} b & d - 2c & 0 & a+b & a+b & 0
\end{pmatrix},
\end{aligned}
\tag{38}
$$

with a, b, c, and d defined by

$$
a = 2\delta(\omega - \omega'), \quad b = 2\left[\frac{\omega\theta(\omega' - \omega)}{\omega'(\omega' - \omega)}\right]_+, \quad c = 2\left[\frac{\theta(\omega - \omega')}{\omega - \omega'}\right]_+,
$$

$$
d = \left[\frac{2}{\epsilon_{\mathrm{UV}}} + 2\log\left(\frac{\mu^2}{\omega}\right) + 1\right]\delta(\omega - \omega'). \tag{39}
$$

Here, the plus distribution is defined by

$$
\int_0^\infty d\omega' \frac{f(\omega')}{[g(\omega')]_+} = \int_0^\infty d\omega' \frac{f(\omega') - f(\omega)}{g(\omega')}. \tag{40}
$$

Cannot solve the corresponding evolution equation in closed form because infinitely many new structure functions with different $\ell_\perp$ weights appear.

Z_S at α_s order for $H \to \gamma\gamma$ case

For the case of $H \to \gamma\gamma$ through b-quark loop, the soft function is sandwiched between $\not{n}_2$ and $\not{n}_1$, which means only the structure function $S_1(\omega)$ survives and does not involve mixing between structure functions

$$
\begin{aligned}
Z_S^{11} &= \delta(\omega' - \omega) + \frac{\alpha_s C_F}{4\pi} \frac{1}{\epsilon_{\text{UV}}} (d - 2a - 2b - 2c) \\
&= \delta(\omega' - \omega) + \frac{\alpha_s C_F}{4\pi} \frac{1}{\epsilon_{\text{UV}}} \Bigg\{ \left[\frac{2}{\epsilon_{\text{UV}}} + 2\log\left(\frac{\mu^2}{\omega}\right) - 3 \right] \delta(\omega' - \omega) \\
&\quad -4\omega \left[\frac{\theta(\omega' - \omega)}{\omega'(\omega' - \omega)} + \frac{\theta(\omega - \omega')}{\omega(\omega - \omega')} \right]_+ \Bigg\}. \qquad (41)
\end{aligned}
$$

Confirms the conjecture in : Z. L. Liu, B. Mecaj, M. Neubert, X. Wang and S. Fleming, JHEP **07**, 104 (2020) at α_s order.

RGE and anomalous dimension

We obtain the renormalization group evolution equation for S_1 by differentiating Eq. (36) with respect to the renormalization scale μ:

$$\frac{d}{d\log\mu}S_1^{\mathsf{R}}(\omega,\mu) = -\int_0^\infty d\omega'\,\gamma_S(\omega,\omega',\mu)S_1^{\mathsf{R}}(\omega',\mu), \tag{42}$$

where the anomalous dimension γ_S is given by

$$\begin{aligned}\gamma_S(\omega,\omega',\mu) &= -\frac{d\log Z_S^{11}}{d\log\mu} \\ &= -\frac{\alpha_s C_F}{4\pi}\Bigg\{\left[4\log\left(\frac{\omega}{\mu^2}\right)+6\right]\delta\left(\omega'-\omega\right) \\ &\qquad +8\omega\left[\frac{\theta(\omega'-\omega)}{\omega'(\omega'-\omega)}+\frac{\theta(\omega-\omega')}{\omega(\omega-\omega')}\right]_+\Bigg\}+\mathcal{O}\left(\alpha_s^2\right).\end{aligned} \tag{43}$$

The large logarithms can be re-summed using the above renormalization group evolution equation.

Outline

Summary

- We have worked out the analyticity structure of the soft-quark function by making use of light-cone perturbation theory.
- The unorthodox momentum routing of the soft-quark function leads to non-local contributions in the renormalization, which makes the renormalization non-trivial.
- We have explained how to renormalize the soft-quark function and confirmed the conjecture given in the literature at α_s order.
- The renormalization group evolution of the soft-quark function is given explicitly, from which the large logarithms can be re-summed.